Brain Connectivity Hypergraphs

Alexander N. Pisarchik
Centro de Tecnología Biomédica
Universidad Politécnica de Madrid
Pozuelo de Alarcón, Madrid, Spain
Immanuel Kant Baltic Federal University
Kaliningrad, Russia
alexander.pisarchik@ctb.upm.es

Natalia Peña Serrano
Escuela Nacional de Estudios Superiores Juriquilla
Universidad Nacional Autónoma de México
Queretaro, Mexico
nattps13@gmail.com

Rider Jaimes-Reátegui
Departamento de Ciencias Exactas y Tecnología
Centro Universitario de los Lagos
Universidad de Guadalajara
Lagos de Moreno, Jalisco, Mexico
rider.jaimes@academicos.udg.mx

2024 8th Scientific School Dynamics of Complex Networks and their Applications (DCNA) | 979-8-3503-9083-4/24/$31.00 ©2024 IEEE | DOI: 10.1109/DCNA63495.2024.10718518

***Abstract*—Hypergraphs are a rapidly developing area of graph theory that has important applications in many fields, including cognitive neuroscience and medicine. In this paper, we review recent advances in the application of hypergraphs to brain connectivity analysis using brain imaging data. We also present our results on the construction of a hypergraph of brain connectivity during visual perception based on the analysis of magnetoencephalography (MEG) data. The hypergraph approach allowed us to identify individual differences in frequency bands, offering deeper insights into the dynamic nature of brain connectivity. Extending traditional graph theory, we defined a functional network connecting different brain regions (vertices) across time segments by generating edge time series that capture temporal fluctuations in connectivity. Using a coherence measure, we created edge time series to illustrate how connections evolve over time. These series contribute to the edge-to-edge functional connectivity network, highlighting hyperedges as connected components in the absolute value functional connectivity network. We identified key features of the brain network across the delta, theta, alpha, beta, and gamma frequency bands and examined interactions among the frontal, parietal, temporal, and occipital lobes in both hemispheres. Our findings support the existence of cortico-cortical interactions, and the resulting hypergraph revealing robust activation patterns in specific brain regions. These results suggest potential integration and multifunctionality within the lobes, providing valuable insights into brain dynamics during visual perception.**

***Index Terms*—hypergraph, brain connectivity, cognitive neuroscience, visual perception, magnetoencephalography (MEG).**

I. Introduction

Hypergraphs have emerged as a powerful tool for studying brain connectivity in recent years [1]–[15]. Unlike conventional graphs, which are limited to modeling pairwise relationships, hypergraphs enable the representation of complex, multi-party interactions among multiple brain regions simultaneously. This approach extends the reach of traditional graph theory by providing a more nuanced and comprehensive view of functional brain networks, capturing the intricate dynamics of connections as they evolve over time. Through hypergraph analysis, researchers can gain deeper insights into how various brain regions interact, adapt, and integrate information during cognitive processes, offering novel perspectives on the organization and functionality of neural networks.

This work was supported by the Russian Science Foundation project No. 23-71-30010.

Understanding brain connectivity in response to a variety of stimuli is critical to uncovering information processing and decision-making mechanisms. Scientists distinguish three types of brain connectivity: structural, functional, and effective. Structural connectivity allows us to build anatomical neural networks, revealing neural communication pathways. Functional connectivity identifies active brain regions with correlated frequency, phase, and amplitude. Finally, effective connectivity infers the dynamic flow of information from functional connectivity data.

In this paper, we review recent advances in applying hypergraphs to study functional brain connectivity and, to the best of our knowledge, present the first hypergraph of functional brain connectivity constructed using magnetoencephalography (MEG) data. By extending traditional graph theory, the hypergraph approach uncovers the functional connectivity network between different brain regions across various frequency bands. Utilizing a coherence measure – a statistical estimate of the correlation between pairs of signals across frequencies – we generate time series of edges that illustrate the evolution of these connections over time. We analyze key features of brain networks in the delta, theta, alpha, beta, and gamma frequency bands, with a particular focus on interactions among the frontal, parietal, temporal, and occipital lobes in both hemispheres. The resulting hypergraph reveals consistent activation patterns in specific brain regions, providing evidence for cortico-cortical interactions. Our findings suggest potential integration and multifunctionality within the lobes, offering new insights into brain dynamics during visual perception.

II. Mathematical Basis

Unlike a traditional graph, where an edge represents a connection between a pair of vertices (nodes), a hypergraph allows for more than two vertices to be connected by a single hyperedge, as shown in Fig. 1.

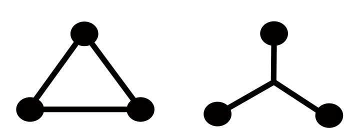

Fig. 1. Examples of a graph (left) and a hypergraph (right) formed by three vertices connected by three edges (left) and one hyperedge (right).

Figure 2 illustrates how a hypergraph of brain connectivity can be constructed. The figure depicts a simple hypergraph, meaning it does not contain empty or multiple edges.

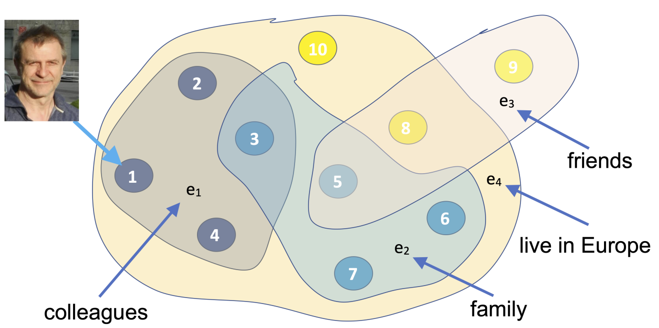

Fig. 2. An example of a simple hypergraph formed by 10 vertices connected by 4 hyperedges.

In this example, the brain's neural network is conventionally divided into 10 areas. When the brain receives a visual stimulus, such as seeing a familiar face (ANP), it activates a neuron (or a set of neurons) in the region corresponding to vertex v_1, which is associated with this person. This neuron then activates other neurons that store information about ANP's colleagues, represented by vertices v_2, v_3, and v_4. Consequently, the hypergraph forms a hyperedge e_1 that connects these four vertices (v_1, v_2, v_3, v_4).

Now, suppose that a colleague associated with v_3 is also a relative of ANP, and thus belongs to a network of relatives associated with vertices v_5, v_6, and v_7, all connected by hyperedge e_2.

Simultaneously, one of ANP's relatives is also a friend of ANP, linking them to the network of friends represented by hyperedge e_3. Additionally, suppose that the individuals associated with vertices $(v_1, v_2, \ldots, v_8)$ and v_{10} reside in Europe, while the person associated with v_9 lives in America. Therefore, the vertices corresponding to those who live in Europe can be connected by hyperedge e_4.

While a graph $\mathbb{G}$ is defined as

$$\mathbb{G} = (\mathbb{V}, \mathbb{E}), \tag{1}$$

where $\mathbb{V}$ is a set of vertices and $\mathbb{E}$ is a set of subsets of size 2 of $\mathbb{V}$, the hypergraph $\mathbf{H}$ in Fig. 2 is composed by a set of vertices $\mathbb{V}$ and a set of hyperedges $\mathbb{E}$ and described as

$$\mathbf{H} = (\mathbb{V}, \mathbb{E}),\ \mathbb{V} = \{v_1, v_2, ..., v_{10}\},\ \mathbb{E} = \{e_1, e_2, e_3, e_4\}, \tag{2}$$

where $e_1 = \{v_1, v_2, v_3, v_4\}$, $e_2 = \{v_3, v_5, v_6, v_7\}$, $e_3 = \{v_5, v_8, v_9\}$, $e_4 = \{v_1, v_2, v_3, v_4, v_5, v_6, v_7, v_8, v_{10}\}$.

A hypergraph is defined by its order and size. The order refers to the number of vertices, while the size denotes the number of hyperedges. In the hypergraph illustrated in Fig. 2, the order is 10, and the size is 4. Additionally, each vertex and each hyperedge is characterized by its degree (Deg). The degree of a vertex v is the number of hyperedges incident to it, whereas the degree of a hyperedge e is the number of vertices incident to it. Mathematically, these degrees can be expressed as:

$$\mathrm{Deg}(v) = \sum_{e \in \mathbb{E}} w(e) * \mathbf{H}(v, e),\ \mathrm{Deg}(e) = \sum_{v \in \mathbb{V}} \mathbf{H}(v, e). \tag{3}$$

In our example, $\mathrm{Deg}(e_1) = 4$, $\mathrm{Deg}(e_4) = 9$, $\mathrm{Deg}(v_2) = 2$, $\mathrm{Deg}(v_9) = 1$, etc.

If a vertex v is covered by two or more hyperedges, we say that these hyperedges are adjacent through v. Similarly, the vertices covered by a hyperedge e are considered adjacent through e. In our example, hyperedges e_1 and e_2 are adjacent through v_3 (denoted as $e_1 \sim e_2$), and hyperedges e_2 and e_3 are adjacent through v_5 (denoted as $e_2 \sim e_3$). Additionally, vertices v_1 and v_2 are adjacent through e_1 (denoted as $v_1 \sim v_2$), while v_2 and v_8 are adjacent through e_4 (denoted as $v_2 \sim v_8$).

A hypergraph can be modified by transforming vertices into edges ($\mathbb{V} \rightarrow \mathbb{E}$) and vice versa. This transformation is called "duality of hypergraphs" and is denoted as $\mathbf{H} = (\mathbb{V}, \mathbb{E}) \rightarrow \mathbf{H}^* = (\mathbb{E}, \mathbb{X})$, where $\mathbb{X} = \{x_1, x_2, \ldots \ldots, x_n\}$, with x_i representing the set of all edges $\mathbb{E}$ incident to vertex v_i. The degree of vertices in a dual hypergraph $\mathbf{H}^*$ is equal to the degree of hyperedges in $\mathbf{H}$, while the degree of the hyperedges remains unchanged from $\mathbf{H}$. This relationship can be expressed as follows:

$$\mathrm{Deg}(v_i) = \mathrm{Deg}(x_i),\ \mathrm{Deg}(e_i) = \mathrm{Deg}(e_i). \tag{4}$$

Additionally, a hypergraph $\mathbf{H}$ can be represented using an incidence graph, an incidence matrix, and a hyperedge weight matrix $\mathbf{W}$.

The incidence matrix $\mathbb{H} = \{0, 1\}^{|\mathbb{V}| \times |\mathbb{E}|}$ is defined as

$$\mathbf{H}[i][j] = \begin{cases} 1, & \text{if } v_i \in e_j, \\ 0, & \text{otherwise.} \end{cases} \tag{5}$$

The incidence graph and incidence matrix of our example are shown in Fig. 3, where the vertical positions represent vertices, while the horizontal positions represent hyperedges.

The weight matrix indicates the significance of each hyperedge in the hypergraph and is given as:

$$\mathbf{W} = \begin{bmatrix} w(e_1) & 0 & 0 & 0 \\ 0 & w(e_2) & 0 & 0 \\ 0 & 0 & w(e_3) & 0 \\ 0 & 0 & 0 & w(e_4) \end{bmatrix} = \begin{bmatrix} 4 & 0 & 0 & 0 \\ 0 & 4 & 0 & 0 \\ 0 & 0 & 3 & 0 \\ 0 & 0 & 0 & 5 \end{bmatrix}. \tag{6}$$

The weight of each hyperedge is located at the corresponding diagonal position of $\mathbf{W}$, i.e., $\mathrm{diag}(\mathbf{W}) = [w(e_1), w(e_2), \ldots, w(e_{|\mathbb{E}|})]$.

III. Recent Advances in Brain Connectivity Hypergraphs

The hypergraph of brain connectivity is a relatively new area of research, with the first publications appearing only a few years ago. Most studies focus on the analysis of functional magnetic resonance imaging (fMRI) data in the resting state [1]–[9], including investigations into various psychiatric

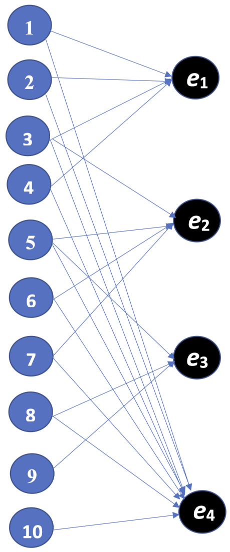

$$\mathbf{H} = \begin{bmatrix} 1 & 0 & 0 & 0 \\ 1 & 0 & 0 & 0 \\ 1 & 1 & 0 & 0 \\ 1 & 0 & 0 & 0 \\ 0 & 1 & 1 & 1 \\ 0 & 1 & 0 & 1 \\ 0 & 1 & 0 & 1 \\ 0 & 0 & 1 & 1 \\ 0 & 0 & 1 & 0 \\ 0 & 0 & 0 & 1 \end{bmatrix}$$

Fig. 3. Incidence graph (left) and incidence matrix (right) for the example in Fig. 2.

disorders [8], such as mild cognitive impairment (MCI) [3], [6], schizophrenia [5], and autism [9], as well as studies on emotion recognition [7]. Hypergraphs have also been constructed for patients with Alzheimer's disease using structural magnetic resonance imaging (sMRI) [10] and other modalities [14]. Furthermore, hypergraphs have been utilized to detect epileptic seizures using intracranial electroencephalography (EEG) data [11]. Noninvasive EEG data have been employed to design hypergraphs for emotion recognition and motor imagery [13]. In addition, MEG data have been used to construct hypergraphs of functional brain connectivity based on event-related coherence during visual perception [15].

One of the earliest applications of hypergraphs in brain connectivity research was conducted in 2017 by American researchers from the University of Pennsylvania [1], who constructed hypergraphs from resting-state fMRI data of 780 adolescents aged 8–22 by analyzing time series data. Later, in 2019, a research group from Tulane University in New Orleans [2] developed a multi-hypergraph learning method based on brain connectivity analysis of fMRI data from 900 subjects aged 8–22.

Hypergraphs based on resting-state fMRI data have also been applied to classify MCI in 91 elderly subjects with a mean age of 74 [3]. Using the Anatomical Automatic Labeling (AAL) atlas, the researchers analyzed time series data recorded from various brain regions. They extracted sliding windows to create a dynamic brain functional network (DBFN) using the Pearson correlation method. From the DBFN, they constructed a hypergraph, which was then used to create a sparse dynamic brain functional network (SDBFN) through hypergraph manifold regularization. This SDBFN allowed them to extract features related to MCI and classify this brain disorder.

Another intriguing application of hypergraphs is in emotion recognition from human facial images. In 2023, researchers from Cincinnati Children's Hospital Medical Center in Cincinnati, OH, constructed hypergraphs for 1400 adolescents aged 8–22 [7]. By analyzing resting-state fMRI time series, they created dynamic weighted hypergraph convolutional networks (dwHGCN) to extract features and classify different emotions. Hypergraphs for emotion recognition were also constructed using noninvasive 62-channel EEG data [12]. The authors analyzed data from 15 subjects who were shown video clips eliciting various emotions.

The hypergraph approach has also been applied to motor imagery classification. Zhu et al. [12] analyzed noninvasive EEG data from 16 subjects in the alpha and beta bands. They achieved a maximum accuracy of 75% in recognizing the lifting of the left and right hands using hypergraphs, whereas non-hypergraph methods yielded an accuracy that was 10% lower.

Hypergraphs are garnering significant interest due to their important applications in diagnosing brain diseases, such as schizophrenia [5], autism spectrum disorder (ASD) [9], epilepsy [11], and Alzheimer's disease [10], [14]. Significant progress in this area has been made by Chinese researchers. For example, Gao et al. [11] constructed hypergraphs using intracranial EEG data from 8 patients to detect and classify epileptic seizures. Additionally, sMRI data from 818 subjects aged 61 to 84 were used to create hypergraphs for the detection and classification of Alzheimer's disease [10]. In 2017, Liu et al. [14] constructed hypergraphs for detecting Alzheimer's disease and MCI using multimodal data, including fluorodeoxyglucose positron emission tomography (PET), MRI, and cerebrospinal fluid (CSF). Their study included data from 99 patients with Alzheimer's disease, 254 patients with MCI, and a control group of 118 conventionally healthy subjects.

These advances in the application of hypergraphs in brain research highlight their promising potential in psychology, medicine, and brain-computer interfaces. However, hypergraphs have yet to be applied to the study of many cognitive functions, such as attention and alertness. In our view, these applications could aid in diagnosing disorders like cognitive disengagement syndrome (CDS) and attention deficit hyperactivity disorder (ADHD).

IV. Hypergraph of Functional Brain Connectivity During Visual Perception

Recently, we analyzed data from 15 subjects recorded during MEG experiments using 306 sensors (102 magnetometers and 204 gradiometers) while they visually perceived a square image with pixels modulated at a frequency of $f_m = 6.67$ Hz. The experiments were conducted at the Center for Biomedical Technology at the Universidad Politécnica de Madrid, Spain. The MEG data were downloaded from https://zenodo.org/record/4408648#.X-72UdYo-Cc.

We calculated the event-related coherence (ERC) relative to the resting state (background) when no stimuli were presented using the following equation:

$$\text{ERC} = \frac{|C_F - C_B|}{C_B}, \tag{7}$$

where C_F and C_B represent the coherence during stimulation and in the absence of stimulation, respectively.

Coherence was measured across four frequency ranges: delta (0–3 Hz), theta (4–7 Hz), alpha (8–12 Hz), and beta (13–30 Hz). The brain was divided into eight areas: the frontal, parietal, temporal, and occipital lobes in both hemispheres. Using these values, we constructed a hypergraph averaged over all participants, as shown in Fig. 4.

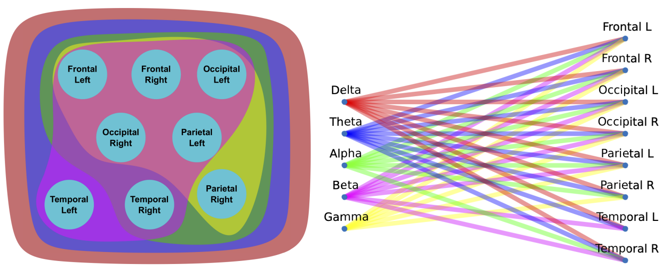

Fig. 4. Hypergraph (left) and incidence graph (right) of functional brain connectivity based on event-related coherence during visual perception. The coherence threshold used is 0.5. The colors represent hyperedges for different frequency bands: red for delta, blue for theta, green for alpha, magenta for beta, and yellow for gamma.

Table 1 presents the degrees of the vertices and hyperedges calculated using equation (3).

TABLE I
DEGREES OF VERTICES AND HYPEREDGES

Vertices	**Deg(v)**	**Hyperedges**	**Deg(e)**
Frontal Left	5	Delta	8
Frontal Right	5	Theta	8
Parietal Left	5	Alpha	7
Parietal Right	5	Beta	7
Temporal Left	3	Gamma	6
Temporal Right	4		
Occipital Left	5		
Occipital Right	5		

V. CONCLUSION

The rapidly developing theory of hypergraph modeling and optimization is still far from complete. Current hypergraph modeling methods lack an evaluation of the quality of high-order correlation modeling, which undermines their credibility. This gap in the literature highlights the necessity for standardized methodologies that can assess and validate the reliability of hypergraph models in capturing the complex dynamics of brain connectivity.

Our findings suggest that each frequency band has a specific coherence threshold; beyond this threshold, significant changes occur in network characteristics such as centrality, shortest path distances, and node degree. Specifically, we observed strong coherence among all eight lobes in the delta and theta bands, but only among six lobes in the gamma band. This variation in coherence underscores the distinct roles that different frequency bands play in facilitating communication between brain regions, suggesting that frequency-specific mechanisms may govern cognitive functions.

Our results support cortico-cortical interactions across scales, with the derived hypergraph revealing robust activation patterns in specific brain regions. This emphasizes the importance of understanding how these interactions contribute to overall brain function and cognitive processes. Additionally, the observed activation patterns may serve as biomarkers for various neurological and psychiatric conditions, providing potential pathways for diagnosis and intervention.

REFERENCES

[1] S. Gu, M. Yang, J. D. Medaglia, R. C. Gur, R. E. Gur, T. D. Satterthwaite, and D. S. Bassett, "Functional hypergraph uncovers novel covariant structures over neurodevelopment," Human Brain Mapping, vol. 38, pp. 3823–3835, 2017.

[2] L. Xiao, J. Wang, P. H. Kassani, Y. Zhang, Y. Bai, J. M. Stephen, T. W. Wilson, V. D. Calhoun, and Y.-P. Wang, "Multi-hypergraph learning based brain functional connectivity analysis in fMRI data," EEE Trans. Medical Imaging, vol. 39, pp. 1746–1758, May 2020.

[3] Y. Ji, Y. Zhang, H. Shi, Z. Jiao, S.-H. Wang, and C. Wang, "Constructing dynamic brain functional networks via hyper-graph manifold regularization for mild cognitive impairment classification," Frontiers in Neuroscience, vol. 15, 669345, 2021.

[4] J. Ji, Y. Ren, and M. Lei, "FC–HAT: Hypergraph attention network for functional brain network classification," Information Sciences, vol. 608, pp. 1301–1316, 2022.

[5] K. Wu, X. Song, and L. Chai, "Graph metrics based brain hypergraph learning in schizophrenia patients," 2022 China Automation Congress (CAC), Xiamen, China, 2022, pp. 3251–3256.

[6] Z. Xi, T. Liu, H. Shi, and Z. Jiao, "Hypergraph representation of multimodal brain networks for patients with end-stage renal disease associated with mild cognitive impairment," Math. Biosci. Eng., vol. 20, pp. 1882–1902, 2023.

[7] J. Wang, H. Li, G. Qu, K. M. Cecil, J. R. Dillman, N. A. Parikh, and L. He, "Dynamic weighted hypergraph convolutional network for brain functional connectome analysist," Medical Image Analysis, vol. 87, p. 102828, 2023.

[8] J. Niua and Y. Dua, "Applications of hypergraph-based methods in classifying and subtyping psychiatric disorders: a survey," Radiology Science, vol. 2, pp. 83-95, 2023.

[9] J. Yang, M. Hu, Y. Hu, Z. Zhang, and J. Zhong, "Diagnosis of autism spectrum disorder (ASD) using recursive feature elimination-graph neural network (RFE-GNN) and phenotypic feature extractor (PFE)," Sensors, vol. 23, p. 9647, 2023.

[10] X. Hao, J. Li, M. Ma, J. Qin, D. Zhang, F. Liu, and for Alzheimer's Disease Neuroimaging Initiative, "Hypergraph convolutional network for longitudinal data analysis in Alzheimer's disease," Computers in Biology and Medicine, vol. 168, p. 107765 (2024).

[11] X. Gao, Y. Zhu, Y. Yang, F. Zhang, F. Zhou, X. Tian, K. Xu, and Y. Chen, "A seizure detection method based on hypergraph features and machine learning," Biomedical Signal Processing and Control, vol. 77, p. 103769, 2022.

[12] M. Li, M. Qiu, L. Zhu, and W. Kong, "Feature hypergraph representation learning on spatial-temporal correlations for EEG emotion recognition," Cognitive Neurodynamics, vol. 17, pp. 1271–1281, 2023.

[13] L. Zhu, Y. Liu, R. Liu, Y. Peng, J. Cao, J. Li, and W. Kong, "Decoding multi-brain motor imagery from EEG using coupling feature extraction and few-shot learning," IEEE Trans. Neural Syst. Rehabil. Eng., vol. 31, pp. 4683–4692, 2023.

[14] M. Liu, J. Zhang, P.-T. Yap, D. Shen, "View-aligned hypergraph learning for Alzheimer's disease diagnosis with incomplete multi-modality data," Medical Image Analysis, vol. 36, pp. 123–134, 2017.

[15] N. Peña Serrano, R. Jaimes-Reátegui, and A. N. Pisarchik, "Hypergraph of functional connectivity based on event-related coherence: Magnetoencephalography data analysis," Appl. Sci., vol. 14, p. 2343, 2024.